LHCb-PUB-2009-018
27 May 2009

From noise to signal – a new approach to LHCb muon optimization

Public Note

Issue 1
Revision 3
Reference LHCb-PUB-2009-018
Created 27 May 2009
Last Modified 30 December 2009

Prepared by A.P.Kashchuk and O.V.Levitskaya

Abstract

The LHCb muon detector has to be exploited at the lowest possible gas gain and operational voltage in order to minimize the charge which will be accumulated during 10 years of the LHCb experiment. The detector lifetime prolongation can be achieved at proper choice of the operational voltage following the optimization technique proposed in this note. An optimization of the LHCb muon system assumes: minimization of the electronics thresholds and the detector gas gain; choice of the working point near a knee of the efficiency plateau at high efficiency, as it is required; stabilization of the signal-to-noise ratio by gas gain stabilization to have constant threshold in primary electrons everywhere in the whole system. The efficiency of each chamber tuned once within bunch crossing time interval will remain constant at the constant gas gain. Cluster size, cross-talks, multi-hits become also constant and minimal at constant and minimal gas gain. It is shown in the note how to reconstruct the noise distribution in each channel and chamber and how to measure precisely the offset and the Equivalent Noise Charge (*ENC*), both of which define the minimal electronics threshold. *ENC* enlargement problem related to threshold increasing at high particle rates is discussed. *ENC* monitoring for each physical channel of the system during the LHCb experiment is proposed as a tool to detect aging effects in the LHCb muon system at the earliest stage and make corrections of the regime.

Contents

Introduction

The muon detector of the LHCb experiment consists of five muon stations (M1-M5) separated by iron filters placed along the beam axis. The LHCb muon is a triggering system crucial for the LHCb experiment: the high-p_T muon candidates ($p_T > 5.0GeV$) are searched. A momentum precision *~20%* is achieved at Level-0 triggering, assuming track from the primary vertex. All 5 stations have to have hits. The tracking stations improve the momentum resolution to *~1%* [1, 2].

The LHCb muon system comprises *1380* chambers covering a total area of *435 m2*: *1368* Multi-Wire Proportional Chambers (MWPC) and *12* GEM-based (Gaseous Electron Multiplier) chambers are arranged in *4* regions R1-R4 around the beam. The LHCb muon system is a pad readout system composed with *20* different chamber types. Each chamber type has a certain pad size, *125k* physical pads (channels) in total. The chambers are two-gap in station M1 and four-gap in stations M2-M5. *1104* chambers of stations M2-M5 have been installed in the pit already more than one year ago. An installation of *276* chambers of station M1 has been completed recently.

Each single-gap MWPC is a fully symmetric chamber with distance between two cathode planes 5mm. Anode wires are the gold-plated tungsten wires arranged with 2mm pitch have diameter 30 μm. CF4-based gas mixture $Ar(40\%)CO_2(55\%)CF_4(5\%)$ is used in MWPC and $Ar(45\%)CO_2(15\%)CF_4(40\%)$ in GEM-chambers.

There is a big progress in software development for setting voltages, testing connectivity, providing time alignment, for measuring efficiency on cosmic rays, etc. However, concerning noise characteristics and setting thresholds nothing new has been appeared during the last year.

A new approach specially developed for optimization of the LHCb muon system and conceptually presented first in ref. [3] is described in this note. This approach is based on minimal electronics thresholds, minimal detector gas gain at maximized efficiency as it is required, stabilized signal-to-threshold ratio which can be implemented by stabilization of the gas gain. An influence of temperature and pressure variations to gas gain has to be compensated by HV tuning automatically. As known, each 100V doubles the gas gain. So, reducing voltage on 100V one reduces time by factor of 2 which is needed to accumulate critical charge. The minimum possible HV will be near a knee of the efficiency plateau.

In such regime of operation one can expect the lowest aging effects resulting prolongation a lifetime of the LHCb muon detector which has to operate at $2\times10^{32}\ cm^{-2}s^{-1}$ luminosity during 10 years of data taking.

Depending on a pad size, each chamber type has a specific detector capacitance C_{det}. This capacitance specifies the Equivalent Noise Charge (ENC) in the front-end electronics which is called below the 'thermal' noise r.m.s. The lowest thresholds are limited by the *ENC* of CARIOCA ASIC [4, 5]. The thresholds are installed by DIALOG ASIC [6]. Both CARIOCA and DIALOG are located on the front-end board called CARDIAC [7]. In case of the LHCb muon system the *ENC* is varied from *0.6fC to 1.9fC* while the sensitivity of CARIOCA is reduced approximately by factor of 2 with C_{det} increasing from *15pF* to *225pF*. As a result, for increasing C_{det} the electronics threshold has to be increased also. The new initiative is to vary the gas gain such that for each C_{det} the ratio signal (gas gain) to noise (threshold) is kept constant in average on the level of 4-5 primary electrons. The gas gain depends on high voltage (HV) applied to the detector, but also on variations of the ambient temperature *T* and pressure *P* via gas density. The HV can be tuned such that effect of *T* and *P* variations are compensated by applied voltage. The gas gain once installed will be kept constant within a given limits by a control system. The gas gain vs. HV has been well measured for the LHCb muon MWPC and fit by Diethorn's parameters, see ref. [8]. So, there is everything to implement stabilization and optimization, as presented here.

In order to find the needed gas gain it is assumed in this note that the threshold w.r.t. signal is constant and corresponds to *4.5±0.5* primary electrons *(p.e.)*, i.e. one accepts missing *(4-5) %* of total ionization equal to *100 p.e./cm* for muons at energy above *6 GeV*, see Appendix.

As expected, with years the *ENC* will be increased due to aging and thresholds have to be corrected in conjunction with correction the operational HV. *ENC* monitoring in each physical channel of the system during the LHCb experiment is proposed in order to detect aging of the system on the earliest stage.

1. Reconstruction of the noise distribution in the LHCb muon system

1.1 Equivalent Noise Charge

A reconstruction of the noise distribution in each individual channel of the system is made with a goal to obtain both offset and *ENC*, i.e. two parameters of the Gaussian distribution in the real conditions for each chamber installed in the pit.

Let's consider parameters of the noise distribution and how each one can be measured.

The equivalent noise charge (*ENC*) is defined as the signal at ratio *S/N=1*. It is specified by the amplifier-shaper of the front-end electronics for a given detector capacitance C_{det}.

The *ENC* is one of the key parameter of the system:

- *ENC* helps to set minimal electronics thresholds and define the minimal gas gain in chambers in order to keep aging effects as low as possible;
- *ENC* is sensitive to other parasitic effects which must be absent or well suppressed;
- *ENC* indicates bad (too noisy) and dead channels which, if found, have to be masked;
- *ENC* is able to indicate aging of the system caused by accumulated radiation during experiment on the earliest stage;
- *ENC* is one of the parameter of the system related to the data quality and has to be periodically re-measured during the experiment.

According to ref.[4] $ENC^{(+)}=1880e+45e/pF$ and $ENC^{(-)}=2200e+42e/pF$ for CARIOCA positive (wire readout) and CARIOCA negative (cathode readout) respectively, see Eq.(1) and Fig.1:

$$ENC = \sqrt{ENC_s^2 + ENC_p^2} = \sqrt{F_s e_n^2 C_{\det}^2 / T_p + F_p T_p i_n^2} \qquad (1),$$

where e_n^2 is the spectral density of the white thermal noise associated with the serial noise, ENC_s , and i_n^2 is the spectral density of parallel noise, ENC_p. The noise components are associated to the voltage noise source and the current source applied to the input of the preamplifier, while F_s, F_p and T_p characterize the next stage, a filter, as illustrated in Fig.2. Fig.2 illustrates also a propagation of the *ENC* from the input to output of the integrator, as a voltage, and so on to the output of the discriminator, as a random counting rate.

The main amplifier together with the shaper and the base line restorer (BLR) are considered here as a filter with a frequency bandwidth extended from f_a to f_b.

Offset is usually a feature of the discriminator. As known, BLR is responsible for large spread of offset levels in CARIOCA chip. *ENC* due to $C_{\det}$ variations (see, for example, ref.[20]) is different from channel-to-channel. How to measure both parameters for each individual channel and reconstruct the noise distribution will be described now.

1.2 Expected rate of zero-crossing

The reconstruction of noise distribution in each channel of the LHCb muon system is made without injection any signal to the input, in contrast to another technique with measuring S-curve, see for example ref.[9].

A threshold scan at zero-signal (only noise presents) gives the raw data. As shown, this will be enough for the reconstruction of the noise distribution in the LHCb muon system [10, 11].

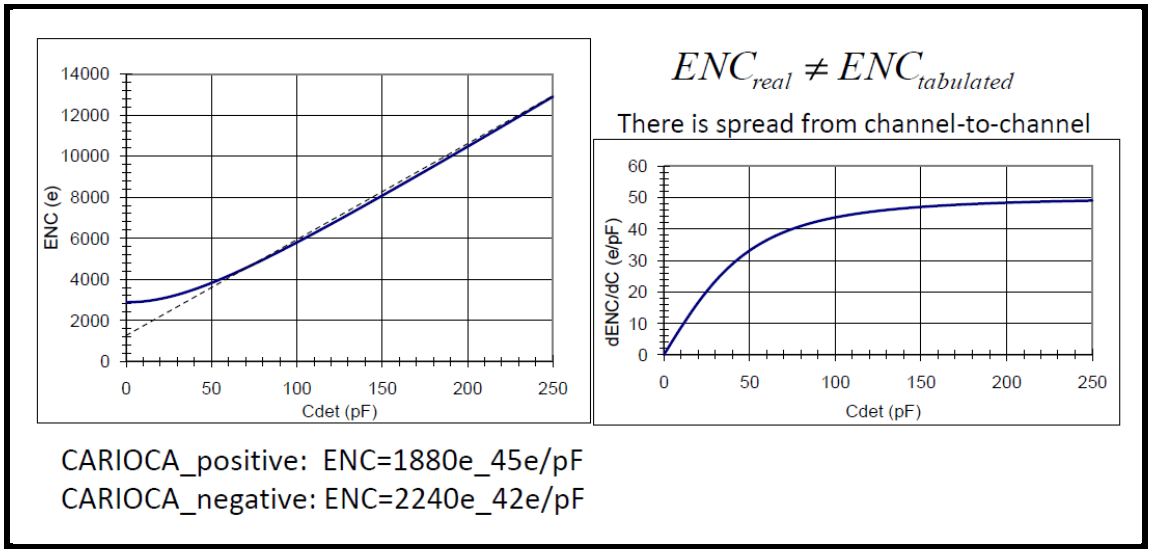

Fig.1. Averaged CARIOCA noise characteristics.

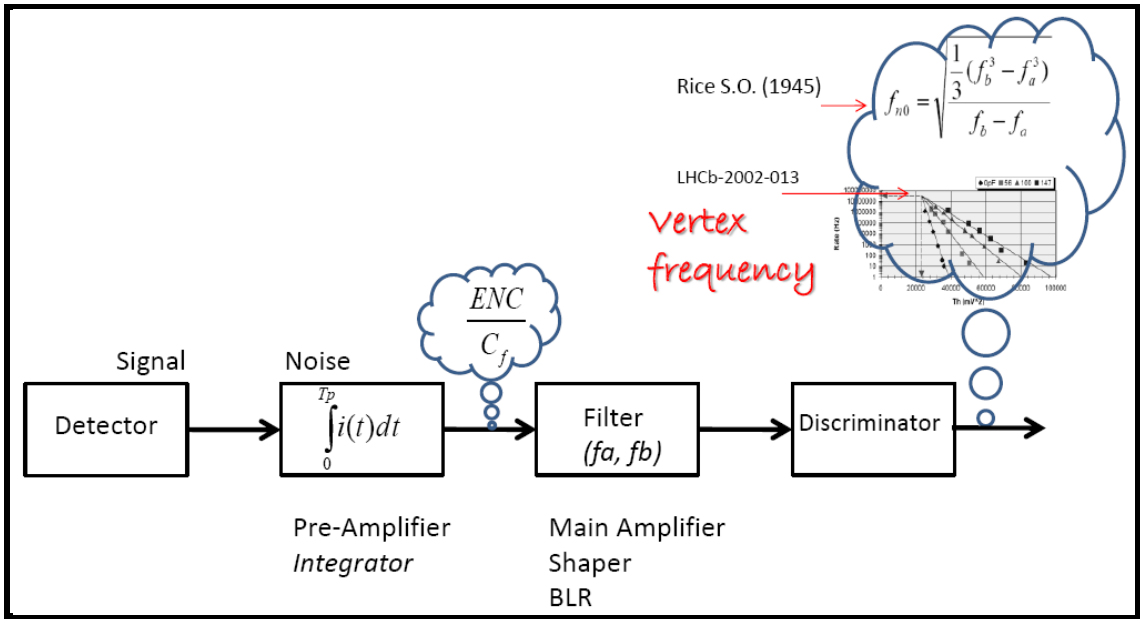

Fig.2. Illustration to ENC propagation and expected rate of zero-crossing.

Then the Rice's formula [11] is used. This formula gives the expected number of zero-crossing for random signal which pass the filter with bandwidth extended from cut-off frequency f_a

to f_b, as illustrated in Fig.2. It is assumed, the Gaussian describes the distribution 'count vs. threshold' with two parameters: mean (offset) and root mean squared, r.m.s (Equivalent Noise Charge). According to Rice's formula, the expected number of zeros per one second of the noise current in a linear system is given by *Eq.(2a)*:

$$f_{n0} = 2\left[\frac{\int_{f_a}^{f_b} f^2 w(f)df}{\int_{f_a}^{f_b} w(f)df}\right]^{1/2} \qquad (2a),$$

where *w(f)* is the power spectral density of the noise current which is constant, i.e. frequency independent, and formula simplified, see *Eq.(2b).*

The rate of zero-crossing in one direction, for example positive one at constant *w(f),* is equal to half of the full counting rate:

$$f_0 = \frac{f_{n0}}{2} = \sqrt{\frac{\frac{1}{3}(f_b^3 - f_a^3)}{f_b - f_a}} \qquad (2b)$$

A charge scale for thresholds will be used in the text below and the expected noise rate for any threshold will be considered as following:

$$f = f_0 \exp\left[-\frac{Q_{th}{}^2}{2ENC^2}\right] \qquad (3)$$

It will be shown, the *ENC* measured in pit well corresponds to *Eq.(1)*, i.e. nothing else except the thermal noise presents there without beam particles. This conclusion is done for randomly taken channels for various chamber types. We work in order to obtain full information from threshold scan raw data for all *125k* channels.

1.3 Centering technique

The centering technique is illustrated in Fig.3 and Fig.4. Basic formula for offset and *ENC* finding is obtained from *Eq.(3)* using log-scale for vertical and quadratic one for horizontal axis:

$$f = f_0 \cdot \exp -\frac{1}{2}\left(\frac{Q_{th}}{ENC}\right)^2$$

$$\log_{10} f = \log_{10} f_0 - \frac{\log_{10} e}{2 \cdot ENC^2} \cdot Q_{th}{}^2 \Rightarrow y = y_0 - \frac{\log_{10} e}{2 \cdot ENC^2} \cdot x \qquad (4)$$

In *Eq.(4) f* is the rate at threshold Q_{th}, f_0 – rate at zero threshold (f_0=*25MHz*) and y_0=7.4.

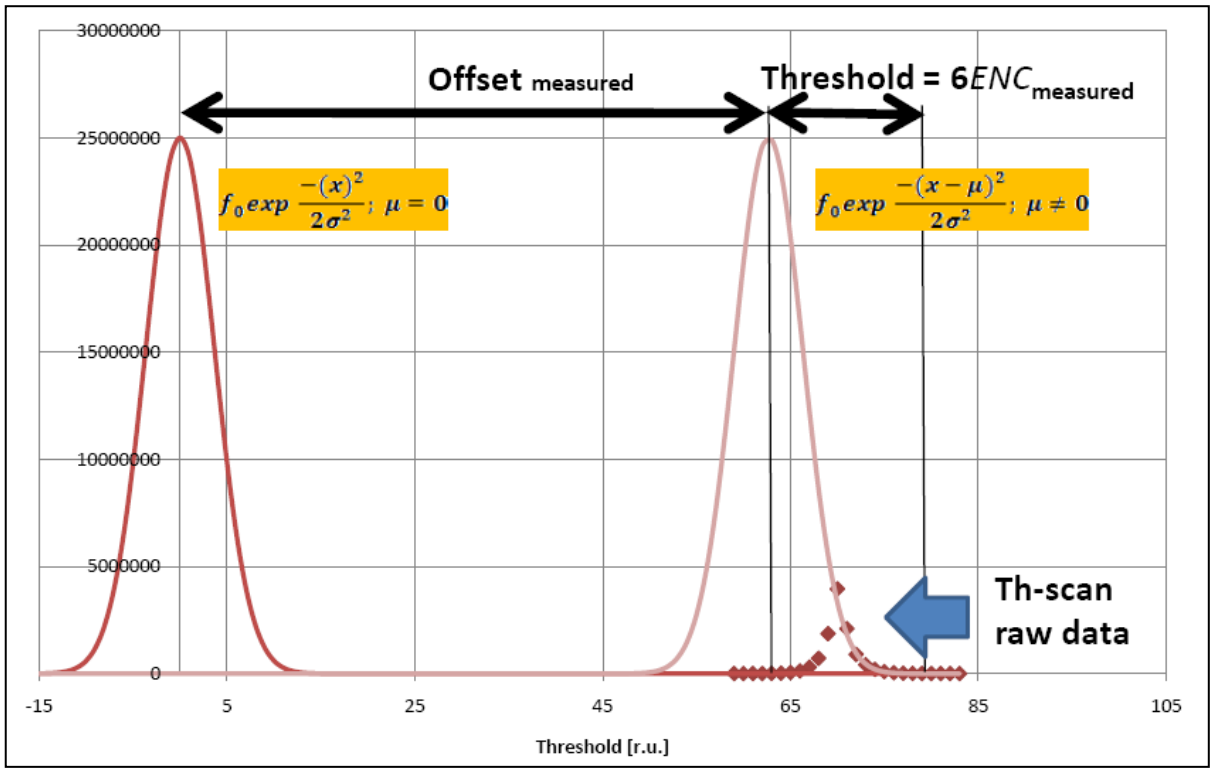

Fig.3. Noise distribution reconstructed from threshold scan raw data. The term 'measured' can be replaced or considered as 'reconstructed' one, but it is found directly from raw data by centering.

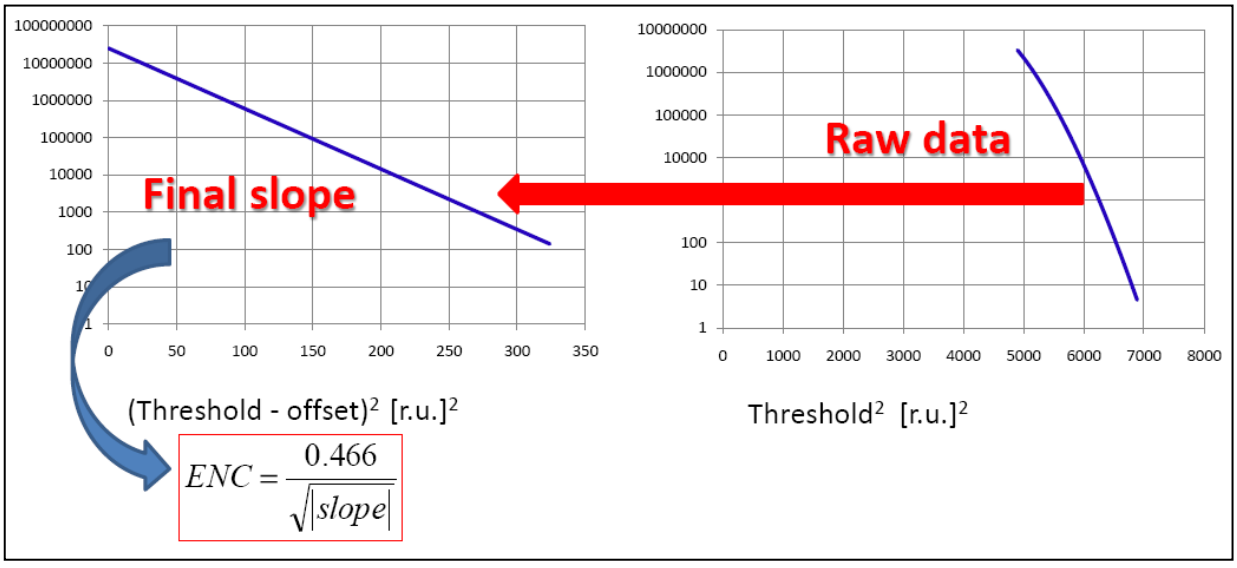

Fig.4. Illustration to centering technique in log-scale vertical and quadratic horizontal axis.

Mathematical shift of the line to left direction from its initial position, shown in Fig.4 and called 'centering technique', is used in order to find offset. The criterion to stop shifting, if the intercept becomes equal to y_0=7.4 at the best straightness of the line. The Equivalent Noise Charge according to the equation *Eq.(5)* is obtained from the slope of this line:

$$ENC = \frac{0.466}{\sqrt{slope}} \qquad (5)$$

1.4 Threshold formula

According to Fig.3 the electronics threshold depends on both parameters of the noise distribution, offset and *ENC*, and can be written in register units (r.u.) as following:

$$Th\,[r.u.] = Offset\,[r.u.] + 6ENC\,[r.u.] \qquad (6)$$

At *6 ENC* the noise count corresponding to zero-threshold, i.e. f_0*=25MHz* (CARIOCA), is suppressed completely. This result can be used as a criterion that measured *ENC* corresponds to tabulated one, i.e. Eq.(1). *5 ENC* is preferable for further minimization of thresholds, but *4ENC* will create too large noise rate.

1.5 FEE channel sensitivity

According to ref.[6], the 8-bit DAC for setting thresholds converts register units to voltage, as 2.35mV/r.u.

In order to represent *ENC* from register units (r.u.) to units of charge one has to calibrate channel. A charge–sensitive preamplifier, as an integrator, transforms the noise charge *ENC* to the voltage similar to signal according to formula Eq.(7) :

$$S = \frac{1}{C_f} \cdot \left(1 + \frac{C_{\det}}{A \cdot C_f}\right)^{-1} \qquad (7)$$

The sensitivity *S* is measured here in units inversed to *pF*, i.e. in *mV/fC*.

Fig.2 shows a set of measurements of *S* made by users. The data follow to analytical expression Eq.(7) for all muon chamber types assuming the feed-back capacitor C_f*=55fF* and open loop voltage gain *A=2700.*

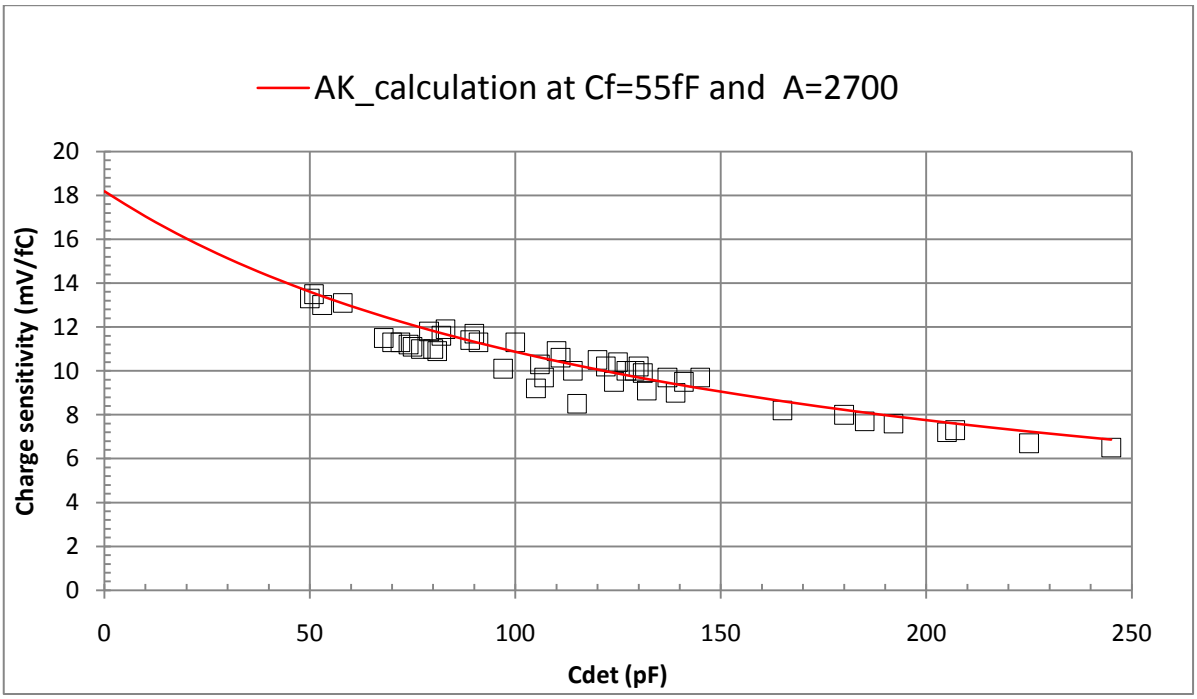

Fig.5. Averaged charge sensitivity as a function of the detector capacitance.

1.6 Examples

ENC directly measured in pit and corresponding thresholds shown in various units for various LHCb muon chamber types are given below, as examples.

M5R4 chamber is the Wire Pad Chamber (WPC) with the largest C_{det}*=225pF* constructed for muon station M5 for region R4. As shown in Fig.6, the *ENC* derivative found here, *42.8e/pF*, is in a very good agreement to expected one for CARIOCA negative which is equal to *42e/pF*. It is a good criterion in order to conclude, that nothing except the FEE thermal noise presents in the pit at present. The threshold and *ENC* expressed in charge units and electrons (here *Th=6ENC=11.4fC=71407e*) can be used to calculate the detector gas gain assuming the noise and signal distributions are separated such that the threshold corresponds to, e.g. 4*p.e.*, and one agrees to loss 5*p.e. (~5%)* from the total ionization of about *100* electron-ion pairs created per cm.

With this requirement for a particular case of the muon chamber M5R4 the gas gain has to be equal at least *73922*, see *Eq.(A2)* in Appendix for more information.

In Fig.7 similar *ENC* measurements are presented for M3R4-chamber with *Cdet=165pF*. It is WPC which has been built for muon station M3 for region R4. The ENC derivative found here,

41.0e/pF, is in a very good agreement to expected one for CARIOCA negative, *42e/pF*. One can conclude, that again nothing except the thermal noise presents in the pit at present. The gas gain has to be equal at least *56025* for the threshold *8.6fC=54000e* corresponding to *4p.e.*

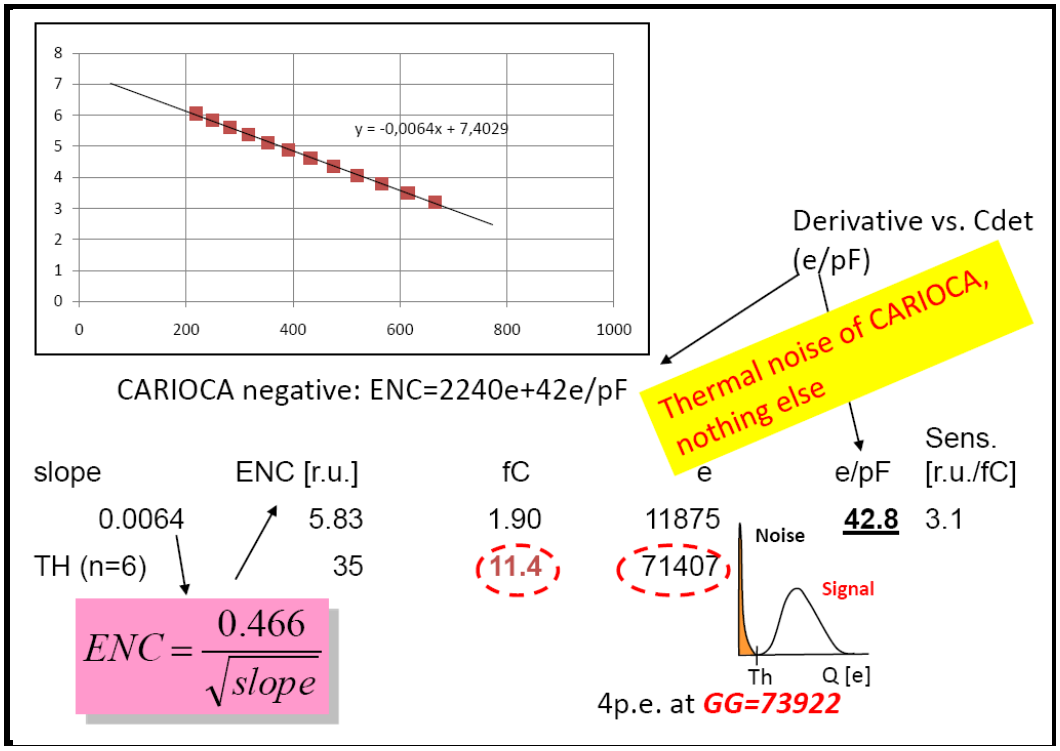

Fig.6. Threshold finding for M5R4 (C_{det}=*225pF*) in various units.

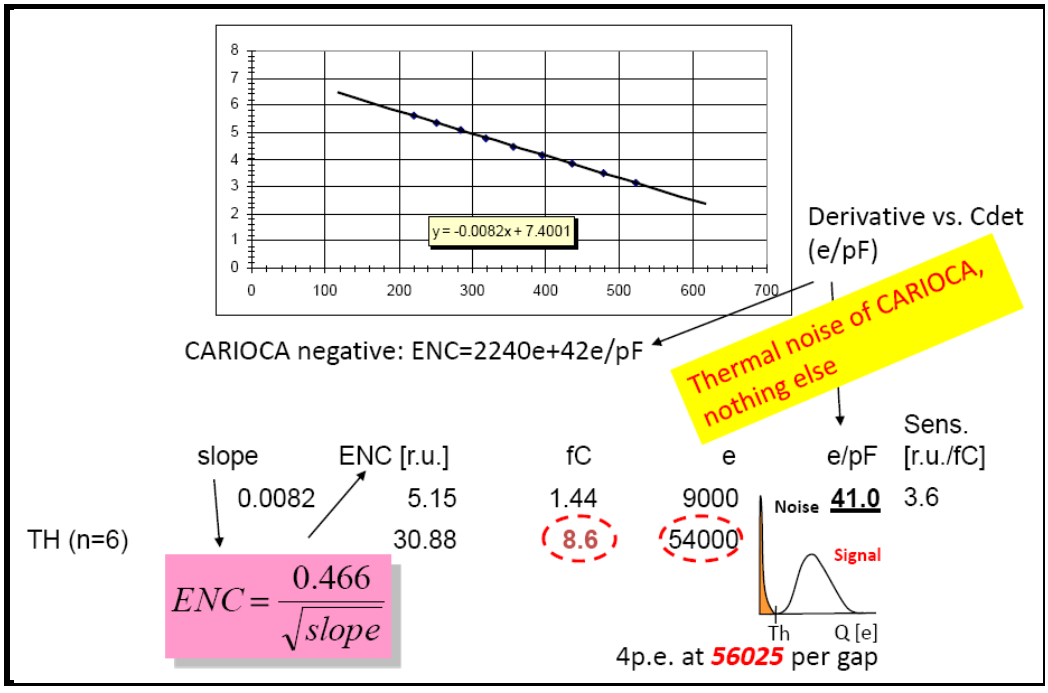

Fig.7. Threshold finding for M3R4 (*Cdet=165pF*) in various units.

In Fig.8 and Fig.9 ENC measurements and calculations related to these measurements made for M5R3 (C_{det}=*145pF*) and M5R1 (C_{det}=*72pF*) are presented. Both chambers are Cathode Pad Chambers (CPC) with single cathode readout (SCRO), i.e. the signal in CPC-SCRO *2* times less than in WPC and the gas gain has to be doubled.

ENC translated from *r.u.* to *fC* are the following: *1.32fC (8250e)* for M5R3 and *0.81fC (5062e)* at sensitivity, as shown in Fig.8 and Fig.9 respectively. In both cases a very good agreement for *ENC* derivative has been obtained, respectively *44.1e/pF* and *44.2e/pF* at expected *45e/pF* for CARIOCA positive. Thresholds *7.9fC=49382e* and *4.8fC=30321e* correspond to *4p.e.* at the gas gain equal to *102713* for M5R3 and 56025 for M5R1 respectively.

As one sees, the gas gain in various chambers has to be different for the same threshold in primary electrons *(p.e.).*

Similar measurements were made for many other channels and chamber types with good results. However, it is still not the full picture of the system with 125k channels and status of the whole system is remaining unknown for authors of this note.

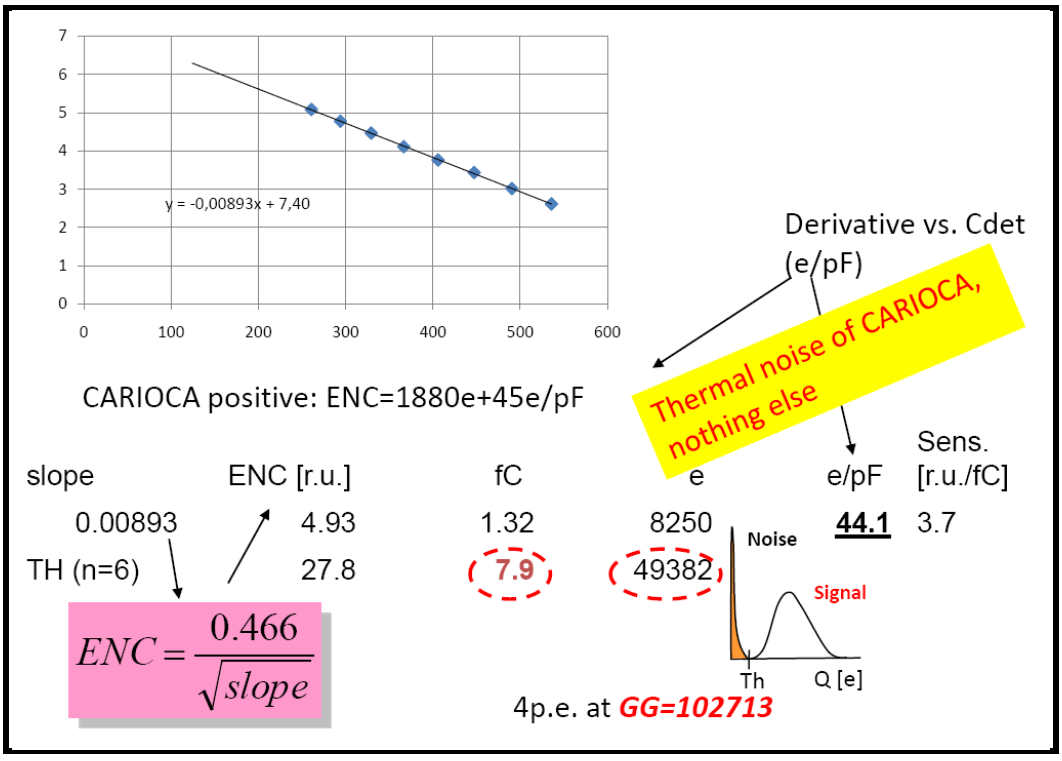

Fig.8. Threshold finding for M5R3 (C_{det}=*145pF*) in various units.

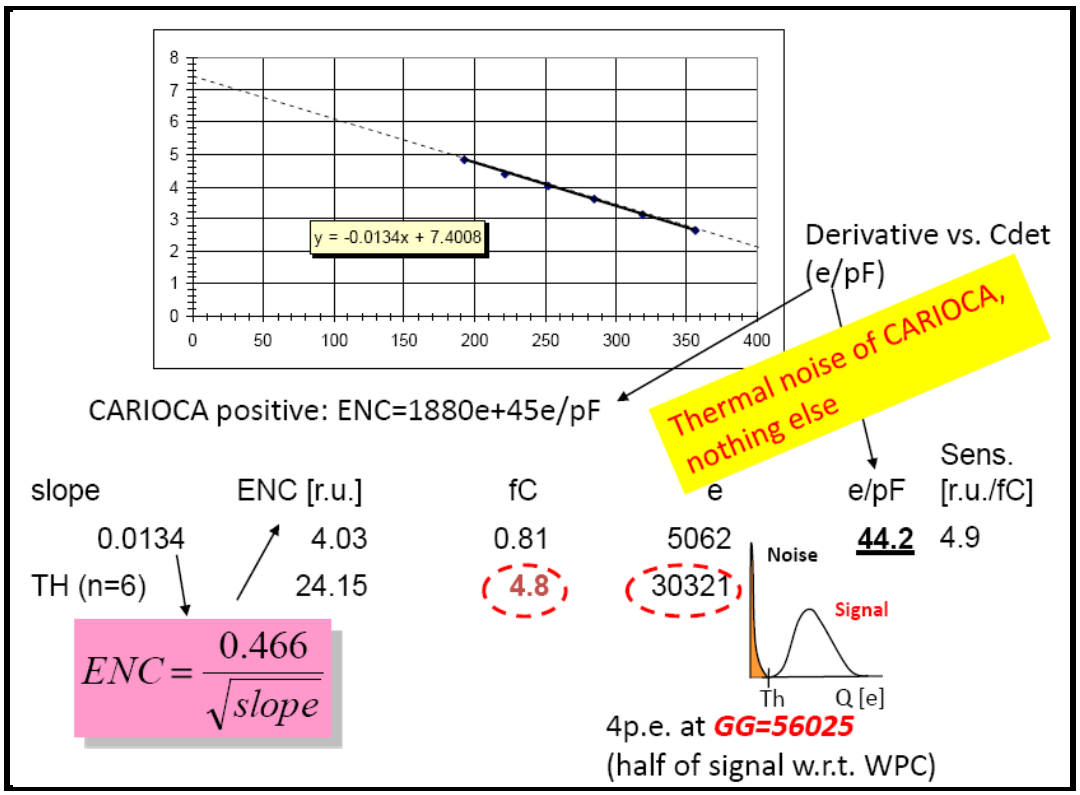

Fig.9. Threshold finding for M5R1 (C_{det}=*72pF*) in various units.

1.7 Critical remarks on threshold formula and thresholds used at present

Unfortunately, the thresholds are installed in pit not according to Eq.(6), but according to Eq.(8) – the empirical formula:

$$Th\,[r.u.] = Max_{raw\_data}\,[r.u.] + Sens\left[\frac{r.u.}{fC}\right]\cdot(Q_{th} - \Delta Q)[\,fC] \qquad (8)$$

Here Max_{raw_data} is the register value corresponding to the maximum of the threshold scan count (it does not correspond to zero-threshold), ΔQ is so called 'minimum detectable charge', see ref. [13, 19].

The formula *Eq.(8)* can be rewritten, as shown *Eq.(8a)*, and then compared to *Eq.(6)*:

$$Th\,[r.u.] = \left\{Max_{raw\_data}\,[r.u.] - Sens\left[\frac{r.u.}{fC}\right]\cdot\Delta Q[\,fC]\right\} + Sens\left[\frac{r.u.}{fC}\right]\cdot Q_{th}[\,fC] \qquad (8a)$$

One can see now that offset is defined in this formula with an error to which 'minimum detectable charge' is known, and the threshold Q_{th} is declared here at unknown *ENC*.

In the formula *Eq.(8)* the parameter 'minimum detectable charge' is usually taken by default, as *3fC* which is incorrect according to Fig.10. Fig.10 also shows that sensitivity and 'minimum detectable charge' are uncorrelated.

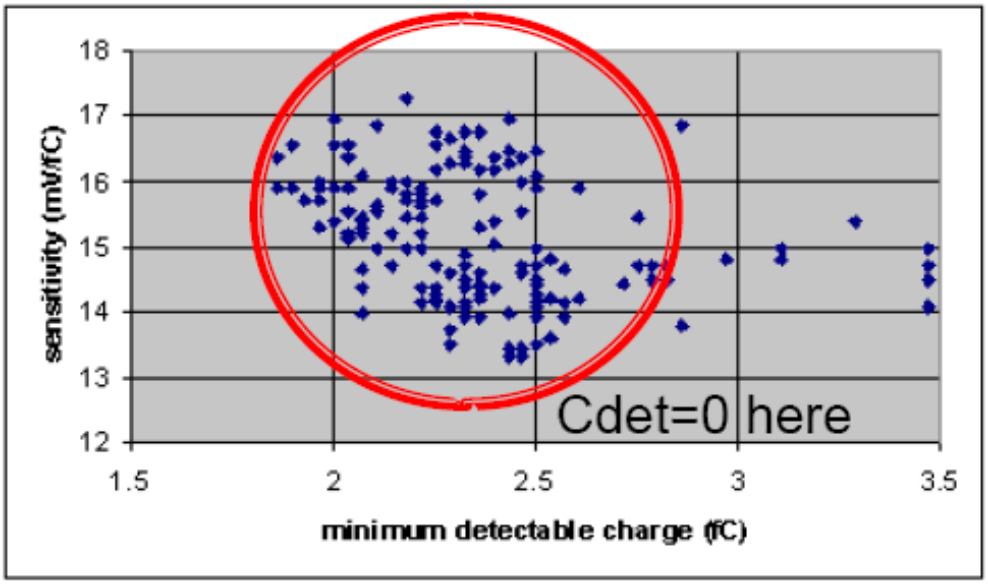

Fig.10. Minimum detectable charge from ref.[13].

In example shown in Fig.11 the systematic error due to bad known 'minimum detectable charge' creates too noisy channel. It is clear that to reduce the number of noisy channels in the LHCb muon system the value of 'minimum detectable charge' has to be reduced (one has to scan this parameter to find an optimum for each channel). It would be the best solution, of course, to replace the formula from *Eq.(8)* to *Eq.(6)* with measured both offset and ENC.

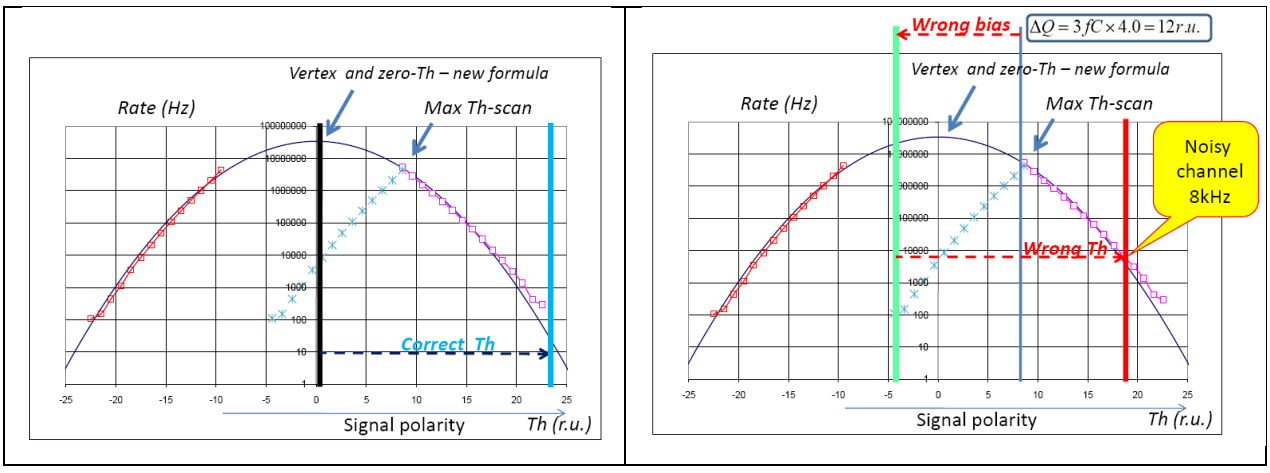

Fig.11.Illustration for setting threshold according to *Eq.(6)* in left and *Eq.(8)* in right.

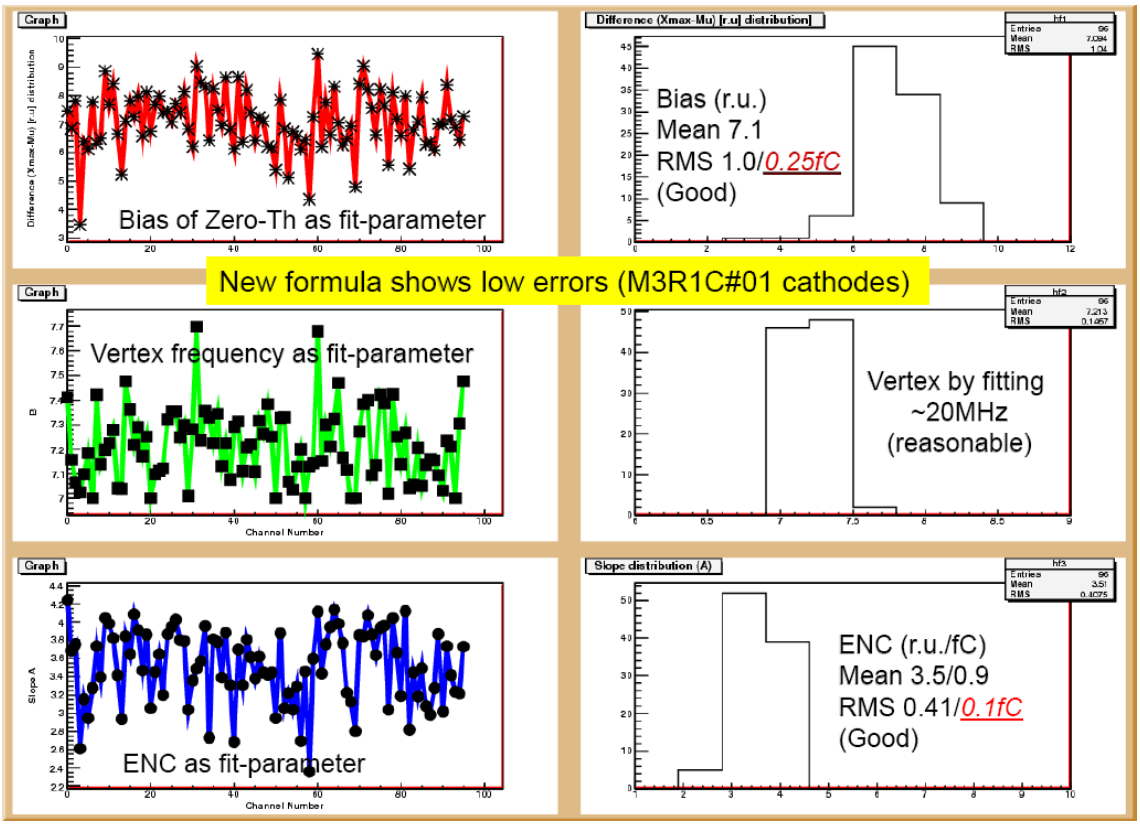

Fig.12. Illustration to low errors in formula *Eq.(6)*.

In the formula *Eq.(6)* both offset and *ENC* are first measured in *[r.u.]* using threshold scan raw data and then inserted to formula. Then the threshold is translated from *[r.u.]* to *fC (e)* for information. Fig.12 illustrates, that errors in formula *Eq.(6)* in all fit-parameters offset (top), vertex frequency (middle) and *ENC* (bottom) are rather low.

The second critical remark is related to electronics threshold values proposed to be used in pit, see Table 1.

Table 1: Low/Median/High thresholds (fC)

Cathodes	**M1**	**M2**	**M3**	**M4**	**M5**
R1	---	7/10.5/14	7/10.5/14	5/7.5/10	5/7.5/10
R2	---	5/7.5/10	5/7.5/10	7/10.5/14	7/10.5/14
R3	---	5/7.5/10	5/7.5/10	7/10.5/14	7/10.5/14
Anodes	**M1**	**M2**	**M3**	**M4**	**M5**
R1	---	10/15/20	10/15/20	---	---
R2	---	10/15/20	10/15/20	---	---
R4	---	10/15/20	10/15/20	12/18/24	12/18/24

Here the so called *High* thresholds are equal to 2 *Low* while *Median* ones equal to 1.5 *Low* and *Median* ones are considered to be installed as a default option. All these numbers are very subjectively defined and default option gives too high thresholds, as it will be compared to optimal thresholds proposed in this note.

Before to compare thresholds the new optimization procedure will be described and discussed.

2. System optimization performed from noise-to-signal

2.1 From minimal electronics threshold to minimal detector gas gain

The LHCb muon system must operate during 10 years at high particle rates with operational gas gain $(0.5\text{-}1.0)\times10^5$ without significant aging [1, 14]. According to this requirement an operation of the LHCb muon system at the lowest possible gas gain at high enough efficiency is mandatory.

FE-electronics (we consider here CARIOCA chip) sets an obvious limit to the minimal threshold. There is no hope of improving this value, unless the errors in finding offset and *ENC* will be minimized as much as possible (see sections 1.6 and 1.7). Electronics thresholds equal to *5ENC* would be preferable to *6ENC*, if the spread of noise characteristics from channel-to-channel allows such choice.

The electronics threshold is related to the detector gas gain, i.e. the signal. The minimal electronics threshold does not mean the minimal threshold in primary electrons *(p.e.)*, see Eq.(A1) in Appendix. For example, the lowest threshold *Th=1p.e.* will require too high detector gas gain, while Th=10p.e. will not allow to get needed efficiency. The optimum threshold in range of *(4-6) p.e.* has been obtained first in ref.[17].

Sequential steps, as shown in Fig.13, have to be performed in order to reach optimum.

The most important and final step after setting minimal electronics thresholds is the final HV finding by a fine time alignment which can only indicate that the needed efficiency has been achieved at minimal gas gain at real particle rate. Environment temperature and pressure have to be recorded during this procedure. These parameters are needed to know as reference for further gas gain stabilization. The starting HV values are given in Table 2 which obtained by calculations for each chamber type using a conception of minimal electronics threshold and minimal detector gas gain corresponding to a given threshold in p.e., as described in the text.

2.2 Working point near the knee of the efficiency plateau

At present, according to [15], the working point WP2 is taken with a safety factor ~100V far away from the knee of the efficiency plateau, see Fig.10. However, each 100V doubles the gas gain and 2 times higher currents will flow through the chambers, as a result, 2 times faster will be reached the critical charge and, in turns, impact to aging. So, one reduces detector lifetime by factor of 2 just simply adding 100V.

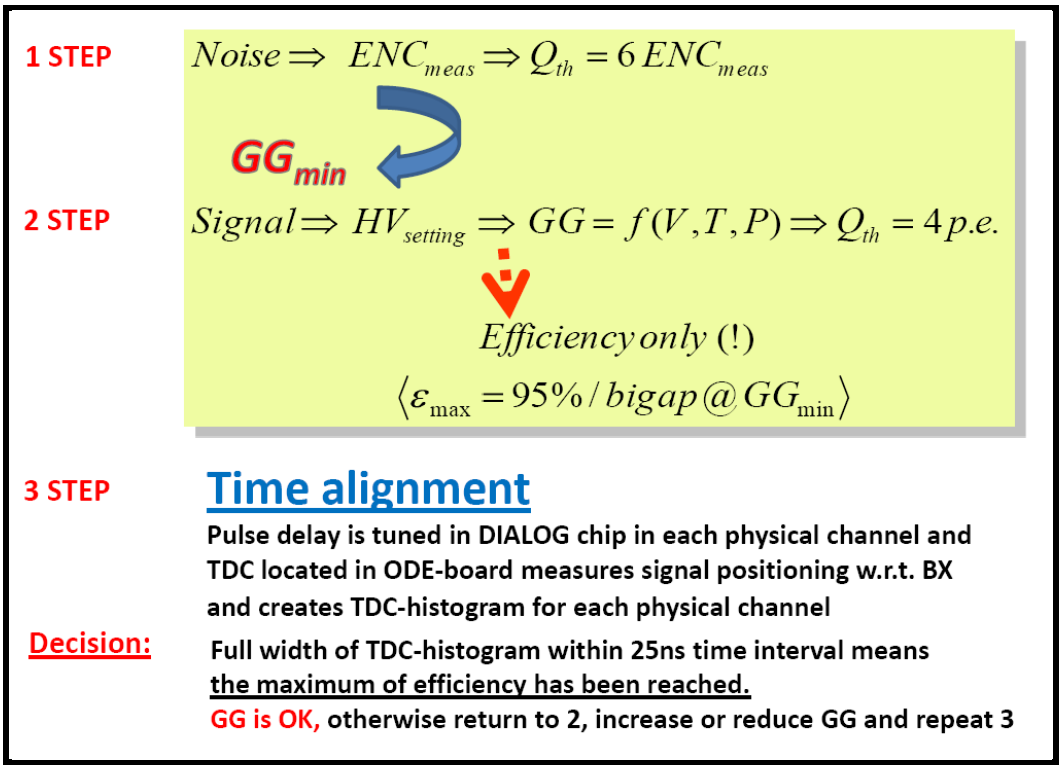

Fig.13. Diagram of steps for optimization of the system from noise-to-signal.

In order to minimize aging effects it would be correct to use working point WP1 in Fig.14, near to the knee. According to requirements [1], the knee must correspond to 95% efficiency for bi-gap and 99.7% for quad gap. In this case taking WP1, one has to provide a regime of operation at which the gas gain (*G* in Fig.14) is constant. This can be achieved, if the gas gain will be stabilized by corresponding HV tuning against temperature and pressure variations. One has keep in mind not only the common environmental parameters *T* and *P* but also the influence of local temperature gradients different in various regions of the system.

There are many other advantages, if the gas gain is constant: then other parameters related to performance optimization as cluster size, hit multiplicity, cross-talks, chamber mean time and rms shown in Fig.15 from ref.[15] as HV-dependent monotonously become constant. Moreover, an

efficiency and time alignment related to chamber mean time and rms tuned once are remaining without change forever.

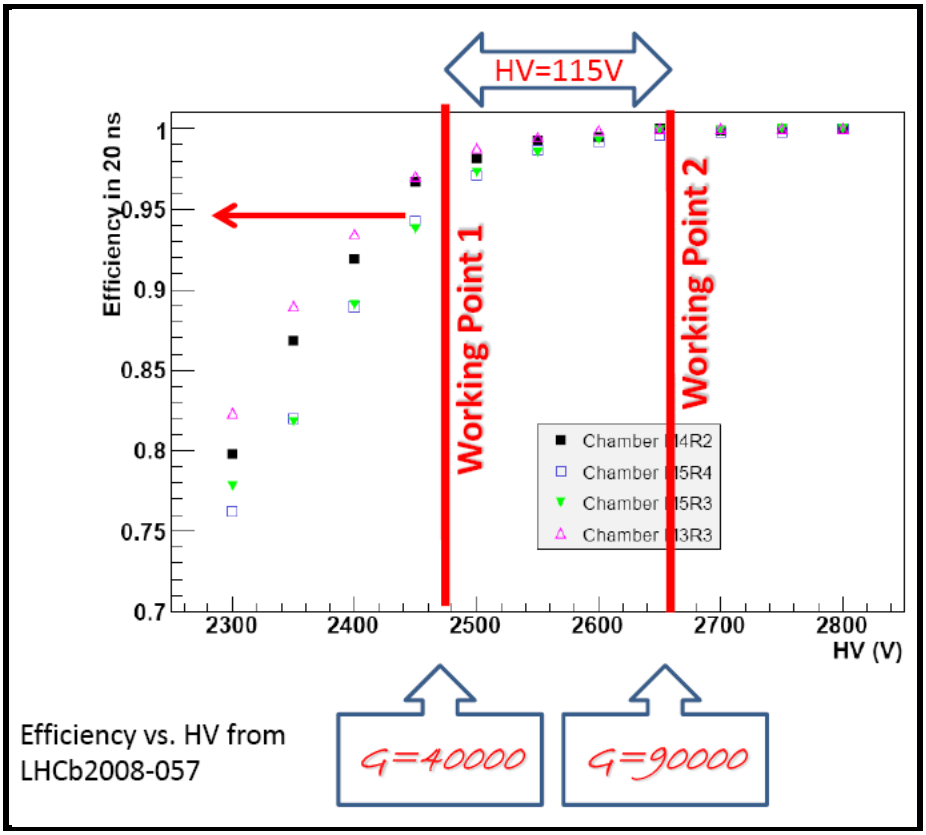

Fig.14. Illustration to choice of the working point near the knee at gas gain stabilization.

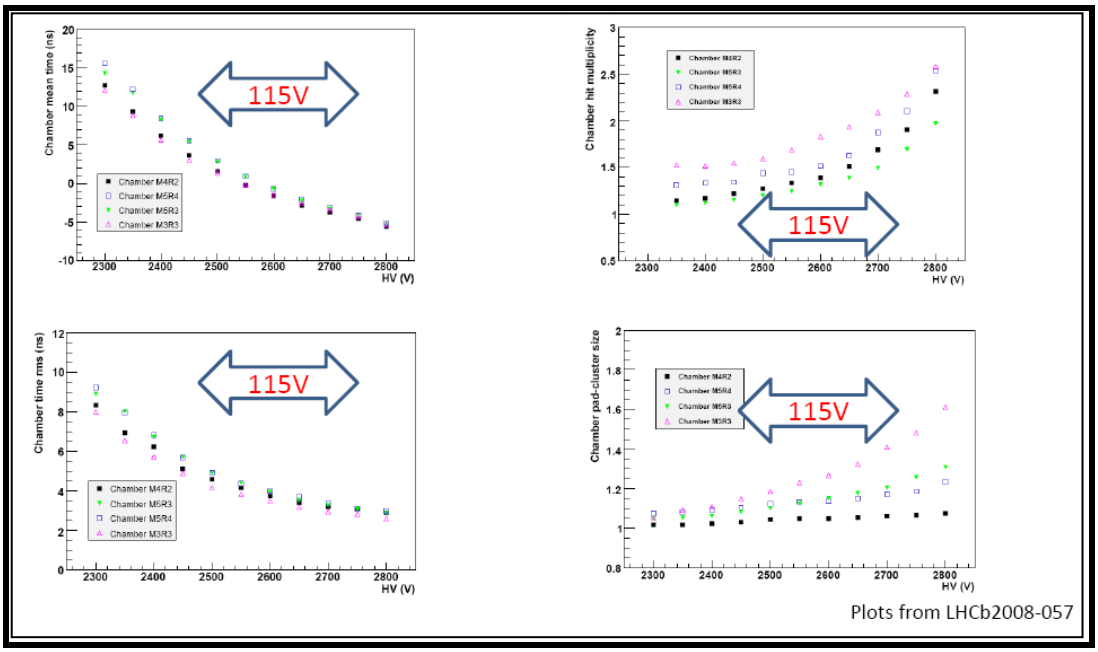

Fig.15. Parameters related to system performance optimization.

2.3 From gas gain to operational voltage

A transition from gas gain to operational voltage will be done using Diethorn's parameters. These parameters have been precisely measured for LHCb muon MWPC filled with the final gas mixture Ar(40%)CO_2(55%)CF_4(5%):

$$G(V,\rho) = \left[V / a \ln\left(\frac{b}{a}\right) \cdot E_{\min}(\rho_0) \frac{\rho}{\rho_0} \right]^{V \ln 2 / \ln\left(\frac{b}{a}\right) \cdot \Delta V} \qquad (9)$$

where E_{min}*=40±2kV/cm,* ΔV*=42±1V* are the best fit parameters for the voltages in a range of 2480-2780V, *a* and *b* are radii of anode wire and cathode respectively, ρ_0 is gas density (reference), see Fig.16 from ref.[8].

2.3.1 Threshold in primary electrons

For a given electronics threshold in *fC (e)* one can decide to which threshold in primary electrons *(p.e.)* it corresponds and estimate the detector gas gain needed for this case, as shown in section 1.6 and Appendix. Then Eq.(9) gives the voltage, as illustrated in Fig.16 and Fig.17.

Fig.16 illustrates an example for M2R4-chamber which shows to which threshold in *p.e.* corresponds some irrelevantly taken threshold in *fC*. So, threshold Q_{th}*=9fC* corresponds to *4p.e.* at *HV=2600V*, but it will corresponds to *6p.e.* at *HV=2520V* and *2p.e.* at *HV=2700V*, while it will be *6p.e.* at *Qth=15fC* and *9p.e.* at Q_{th}*=20fC* according to Table 1. Thus, one has to specify the detector gas gain, talking on electronics threshold, as it is given below in Table 2.

2.4 Table of the operational parameters for LHCb muon system

As shown in Fig.17, *±2.5%* variations of *T/P*-ratio give *~40V* shift in HV and even much more, according to *Eq.(10)* from ref. [8], at larger *T/P*-ratio variation.

$$V \sim 770 \left(\frac{\Delta P}{P} - \frac{\Delta T}{T}\right) = 115V@15\% \qquad (10)$$

For example, 100V corresponding to *~15%* variation will be possible in the inner-most MWPC. It is well known that power dissipation on FEE-boards depends on switching frequency of CMOS-transistors, i.e. on particle rate. This effect has to be taken into account also in ENC finding, see Table 2 and section 3.2..

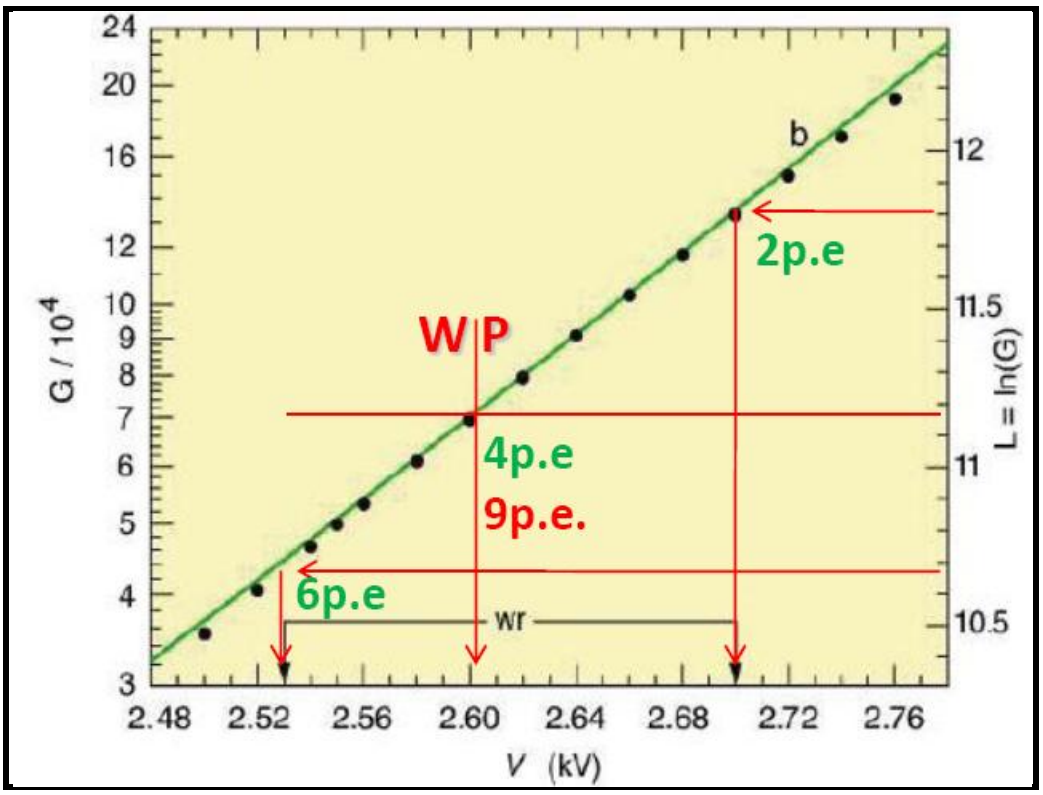

Fig.16. Diethorn's plot for LHCb muon MWPC from ref.[8].

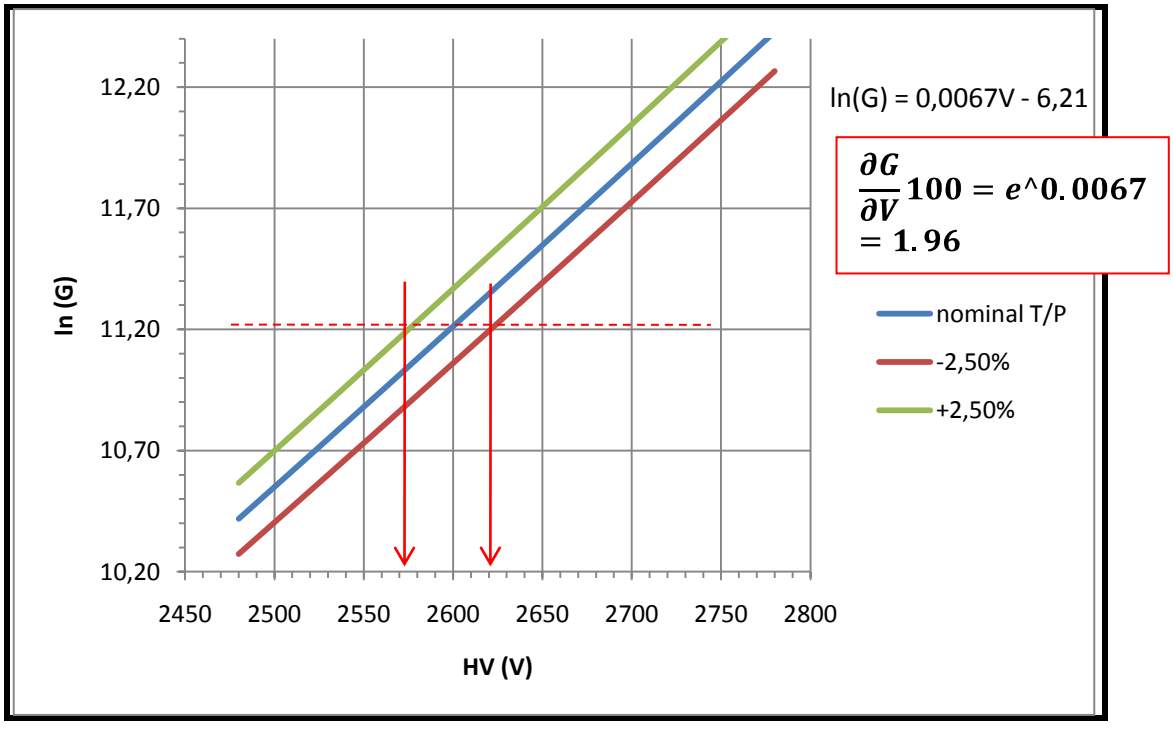

Fig.17. Impact of the T/P-ratio variations to HV at a given gas gain.

As one can see from Fig.17, each 100V doubles the gas gain. It is not easy to make precise calculation of the HV for a given gas gain with such a strong influence of the environment to the gas density ρ via T and P variations. It has to be mentioned that Diethorn's parameters have been measured for one chamber only. Various chambers due to design imperfections have spread in the gas gain. But if calibrate method to existing experimental data for some chamber type, one can then extrapolate results to all other chambers (as done in Table 2). Table 2 summarizes the main parameters which are needed to define electronics thresholds, detector gas gain and estimate operational HV using *Eq.(9).* In Table 2 electronics thresholds are taken as *6ENC* at zero offset (assuming that offset is precisely measured). Attention: *ENC* presented in ref. [16] are wrong with systematic disagreement to *ENC* derivative, as shown in Table A1 in Appendix, and for this reason are useless and cannot be used neither for threshold estimation in *ENC*-units nor for threshold setting. Tabulated *ENC* values have to be used instead in this case. Very good agreement between measured and tabulated *ENC* has been already illustrated in section 1.6. The detector gas gain has been found in Table 2 for each chamber type with an assumption that threshold corresponds to *4.5±0.5p.e.* The operational HV for each chamber type is shown with the range of *±20V* which corresponds to *±0.5p.e.* If compare to ref.[3], HV were reduced by increasing threshold in *p.e.* and taking 12% fraction (instead of 10%) of charge collected during T_p according to Eq.(A1) in Appendix. Now there is an agreement to measurements made on Cosmic Ray stand in Roma1 for chambers M5R3, M4R3 and M4R2, but disagreement on *90V* is obtained for M3R3 (*5ENC* threshold does not enough to explain such deviation w.r.t. ref [15], but this deviation is easy explained by threshold *9p.e.*). Similar disagreement *60V* with beam tests of M3R1-chamber can be found [19], while a good agreement between calculation and measurement is obtained assuming threshold *6p.e.* in measurements. An agreement to working range for M5R4 which starts from *2570V* is also good. The data in Table 2 are proposed as a baseline or guideline solution for application in pit before the LHCb muon system will be optimized completely. At present time the muon system is running at HV=2650V everywhere which is bad for inner-most MWPCs from aging point of view. The final operational voltages have to be found experimentally on the real particle rates and final LHC clock, as it is described in section 2.1 (even to reduce HV given in Table 2, if possible). The HV corresponding to a knee of the efficiency plateau are the best for a maximum prolongation of lifetime of the chambers. In order to use a working point near the knee, the gas gain stabilization becomes mandatory.

Table.2. Baseline solution for thresholds, gas gain and HV for the LHCb muon system.
Notes: In the combined readout MWPC the gas gain and HV are defined by cathodes with larger C_{det};
Double thresholds found for cathodes have to be used in anodes in these chambers;
The lower HV in measurements (green) are simply explained by higher thresholds in (*p.e.*);
If local temperature on FE-boards is increased by power dissipation, the ENC is increased also increasing an effective threshold, as shown (red) in M1R1 and M1R2 - most dense regions in the muon detector.
WP and WR are the Working Point and the Working Range respectively [15].
Correct offset and tabulated ENC are assumed here in calculations.

	Measurements				Calculations				Experimental data			
Chamber type	Cdet (pF)	S (mV/fC)	ENC (fC)	Th= 6ENC (fC)	Th= 6ENC (e)	GGmin 4.5±0.5(p.e)	ln(GG)	HV range 4.5±0.5p.e (V)	CERN GIF/ PS (V)	CR_WP (LowTh) (V)	CR_WR (LowTh) (V)	Double T by local power dissipation
M1R1GEM	15	20	0,4	2,4	15000	5000 3p.e. 4.5p.e.		1280 3p.e. 4.5p.e.				+high rate ENC+Δ
M1R2_DCRO	53±10	13±0,5	0,67 (0,8)	4 (4,8)	25290 (30000)	21637 6p.e. (27700)	10,00 (10,3)	2420±20 6p.e. (2460±20)				+high rate ENC+Δ
M1R3_DCRO	82	11,5	0,9	5,4	33750	28875	10,27	2460±20				
M1R4W	122	9,8	1,2	7,2	45000	38500	10,56	2510±20				
M2R1_DCRO	124±10	9,5±0,5	1,20	7,2	45000	38500	10,56	2510±20				
M2R1W	72±10	11,5±0,5	0,6	14		38500	10,56	2510±20				
M2R2_SCRO	105±10	9,2±0,5	1	6	37500	64167	11,07	2590±20				
M2R2W	85±10	10,5±0,5	0,7	12		64167	11,07	2590±20				
M2R3_SCRO	106	10,3	1,1	6,6	41250	70583	11,16	2600±20				
M2R4W	165	8,4	1,5	9	56250	48125	10,78	2550±20				
M3R1_DCRO	130±10	7,6±0,5	1,2	7,2	45000	38500	10,56	2510±20	2450 6p.e. [13]			
M3R1W	84±10	11,2±0,5	0,6	14		38500	10,56	2510±20	2450 [13]			
M3R2_SCRO	115±10	8,5±0,5	1,1	6,6	41250	70583	11,16	2600±20				
M3R2W	90±10	10,2±0,5	0.7	12		70583	11,16	2600±20				
M3R3_SCRO	114	10	1,1	6,6	41250	70583	11,16	2600±20	2550 [18]	2510 [15] 9p.e.	2500- 2520 [15]	
M3R4W	185	8	1,6	9,6	60000	51333	10,85	2560±20				
M4R1_SCRO	72±10	11,3±0,5	0,8	4,8	30000	51333	10,85	2560±20				
M4R2_SCRO	139	9	1,3	7,8	48750	83417	11,33	2630±20		2660 [15]	2520- 2800 [15]	
M4R3_SCRO	139	9	1,3	7,8	48750	83417	11,33	2630±20		2650 [15]		
M4R4W	205	7,5	1,7	10,2	63750	54542	10,91	2560±20				
M5R1_SCRO	75±10	11,1±0,5	0,8	4,8	30000	51333	10,85	2560±20				
M5R2_SCRO	139	9	1,3	7,8	48750	83417	11,33	2630±20				
M5R3_SCRO	145	8,8	1,3	7,8	48750	83417	11,33	2630±20		2630 [15]	2570- 2700 [15]	
M5R4W	225	7,2	1,9	11,4	71407	107110	11,58	2660±20		2660 3p.e.	2570- 2750 [15]	

3. Noise enlargement problem at high rates

3.1 Cross-talks

At high rates on can expect both gas gain reduction due to space charge and *ENC* enlargement with respect to the thermal noise due to cross-talks. If *N* channels are coupled and a part of the signal penetrates from one channel to other ones, then there is a rate magnification effect by factor *N* and such effect can be considered as an additional random noise.

The maximum number of coupled channels at so called Z-talks due to non-zero common impedance located between detector and FE-electronics ground points, as shown in Fig.18 (right): all channels involve in 'talk'. The effect is less at lower detector gas gain and at low rates, as for example has been illustrated in ref. [19, 20].

Fig.18 shows Z-talks vs. threshold measured in M5R1-chamber at GIF (CERN) at rates of gammas 5-times above the upper limit for such chamber which is expected in the LHCb experiment [20]. Cross-talks are increased exponentially with reduction of the threshold. However, effect starts to be relevant at electronics thresholds below 6fC (here *ENC* thermal included).

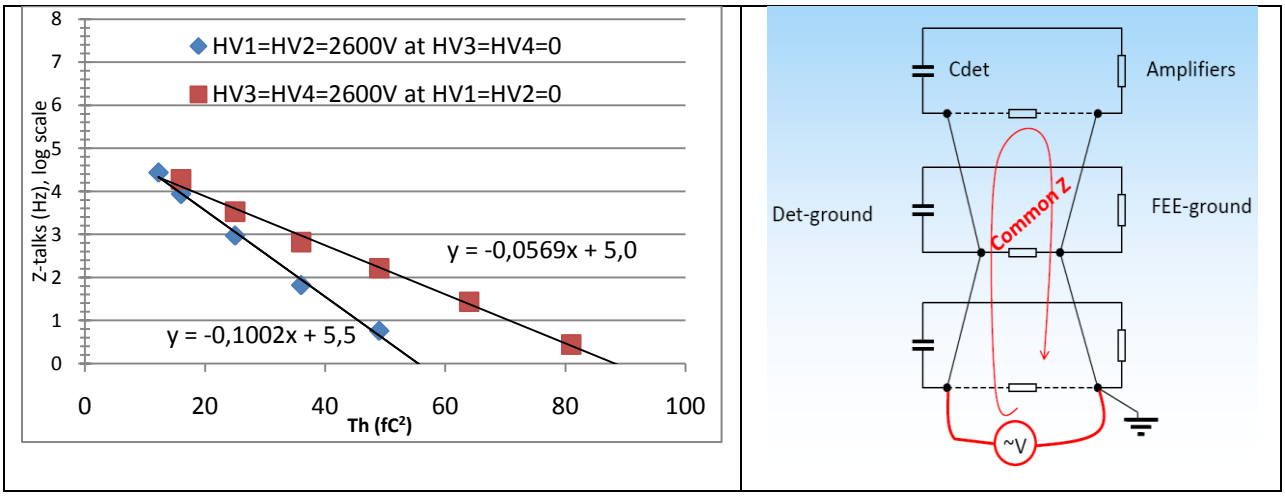

Fig.18. Cross-talks (Z-talks) measured in M5R1 on GIF at rates 5-times above limit rate for M5R1 (left). Common impedance in ground between the detector and electronics ground (right).

Cross-talks are pick-ups and cannot exceed the rate of the source. In our example reduction the rate *5* times (to get expected rate for M5R1) will change the intercept fit-parameter from *5* to *1* in Fig.18, where the frequency 200kHz gives 5.3 in log-scale.

Similar measurements were made for all the inner-most chambers, see ref. [20].

Very similar effects of cross-talks were observed in pit lowing thresholds and increasing noise rates in the system, see for example ref. [21].

One can conclude from these measurements that no reason to increase electronics thresholds due to cross-talks at least at present time.

3.2 ENC enlargement by local power dissipation

ENC depends on temperature according to *Eq.(1)*, because $e_n^2 = 4kTR_s$ and $i_n^2 = 4kT/R_p$ are proportional to temperature T (k – Boltzmann constant, R_s and R_p are serial and parallel noisy resistors). The temperature depends on power dissipation on *ASIC* which is already 2-times higher for the dense regions. But at high particle rates it will be increased proportionally to switching rate of CMOS-transistors. It is very bad effect especially for M1R1 and M1R2, where both rate and electronics density are the highest in the LHCb muon system.

`In Table *2* such *ENC* enlargement effect is highlighted for M1R1 and M1R2 as increased thresholds in primary electrons. In order to reduce thresholds in p.e. one has to add HV which impacts to aging (values in parentheses in Table 2).

4. On ENC monitoring during experiment starting from the first beams

The LHCb experiment has to be able to work many years and ENC has to be periodically re-measured during the experiment. This can be done at any interruption of data taking, for example, once per month. The raw data of threshold scan have to be collected in Data Base and processed off-line with the goal of reconstruction of the noise distribution and measuring both offset and ENC in each individual channel of 125k channels. Such *ENC* monitoring with systematic measurements of both parameters of the noise distribution and comparison to initial values can help to detect aging effects on the earliest stage of its development and make correction in operation of the LHCb muon system. Self-sustaining discharges in some chambers and also emission induced by particles (both phenomena are expected in reality, see ref. [22]) can be detected starting from the first beams, then, as expected, disappear at further detector conditioning. These processes have to be under very careful control. To save chambers is the most important task especially at the beginning of the experiment.

Plot *ENC* vs. time presented for each channel, hopefully, will give information on ‘health’ of the system with years of data taking.

Conclusion

As one can find from ref.[26], the current status and characteristics of the LHCb muon system obtained with the 2008 cosmic runs are far from ideal. And what can be expected and measured at absolutely un-optimized regime and setup? So, the main activity for system optimization will take place with beam during the first year. However, what can be done without beam is the noise study in the real setup and minimum achievable electronics thresholds related to thermal noise only.

One has to exploit the LHCb muon detector at the lowest possible gas gain and voltage in order to minimize the accumulated charge during *10* years of the running LHCb experiment. A new approach to optimization of the LHCb muon system from noise to signal has been described in this note and first presented conceptually in ref. [3]. More accurate calculations of the gas gain and operational HV were made in this note using the existing experimental data for part of chamber types. An optimization of the LHCb muon system assumes: minimization of the electronics thresholds and detector gas gain, choice of the working point near the knee of the efficiency plateau at stabilization of the signal-to-noise ratio by gas gain stabilization in order to have constant thresholds in primary electrons everywhere during long-term data taking run. The efficiency of each chamber tuned once by a time alignment remains constant at the constant gas gain. Cluster size, cross-talks, multi-hits become constant and minimal at constant and minimal gas gain. It is shown in the note how to reconstruct the noise distribution in each chamber and to measure precisely the offset and the Equivalent Noise Charge (*ENC*), both of which specify the minimal electronics threshold. *ENC* enlargement problem related to threshold increasing at high particle rates is discussed. *ENC* monitoring for each physical channel of the system during the LHCb experiment is proposed in order to detect aging of the LHCb muon system at the earliest stage. 1.5-2 times in the detector lifetime prolongation can be achieved following to optimization of the LHCb muon system proposed in this note.

Acknowledgements

Authors thank Igor Smirnov for useful discussions, and would like to thank B.Schmidt and G.Passaleva for continuous interest on further optimization of the LHCb muon system and support the idea of *ENC* monitoring during the LHCb experiment.

References

[1]
LHCb Muon System, Technical Design Report, CERN/LHCC 2001-010, 28 May 2001
http://lhcb-muon.web.cern.ch/lhcb-muon/TDR/TDR_pres_part1.ppt

[2]
The LHCb Detector at the LHC
2008 JINST 3 S08005
http://www.iop.org/EJ/article/1748-0221/3/08/S08005/jinst8_08_s08005.pdf?request-id=4cd6823e-81b1-4d9e-b531-aa426ecfad1e

[3]
A.Kashchuk and O.Levitskaya
http://indico.cern.ch/getFile.py/access?contribId=8&resId=1&materialId=slides&confId=58893

[4]
CARIOCA ASIC
http://indico.cern.ch/getFile.py/access?contribId=s1t2&resId=0&materialId=0&confId=a03311

[5]
Walter Bonivento on behalf of the LHCb muon collaboration
The front-end electronics of the LHCb muon system
http://lhcb-doc.web.cern.ch/lhcb-doc/presentations/conferencetalks/postscript/2005presentations/W.Bonivento.pdf

[6]
DIALOG ASIC
http://doc.cern.ch//archive/electronic/cern/others/LHB/internal/lhcb-2003-016.pdf

[7]
CARDIAC board
http://indico.cern.ch/getFile.py/access?subContId=0&contribId=s1t1&resId=1&materialId=0&confId=a054562

http://indico.cern.ch/getFile.py/access?contribId=s1t0&resId=0&materialId=0&confId=a054562

[8]
D.Dané, G. Penso, D. Pinci and A. Sarti
Detailed study of the gain of the MWPCs for the LHCb muon system
Nuclear Instruments and Methods in Physics Research A 572 (2007) 682–688
http://www.sciencedirect.com/science?_ob=ArticleURL&_udi=B6TJM-4MPKBSH-6&_user=8158783&_rdoc=1&_fmt=&_orig=search&_sort=d&_docanchor=&view=c&_acct=C000027764&_version=1&_urlVersion=0&_userid=8158783&md5=df0e358ad9092748ffc4d2d9a570b93f

[9]
A.Pellegrino, et al. OT FE-Box Test Procedures
LHCb-2007-122
http://cdsweb.cern.ch/record/1064040/files/lhcb-2007-122.pdf

[10]
Procedure for determination and setting of thresholds implemented in the LHCb Muon system ", LHCb-2008-052, Geneva, CERN, 2008.
A.Kashchuk, R.Nobrega and A.Sarti
http://cdsweb.cern.ch/record/1131816/files/LHCb-2008-052.pdf

[11]
Pre-installation Tests of the LHCb Muon Chambers
B.Schmidt, *et al.* IEEE Nuclear Science Symposium
Dresden, Germany, October 22sd, 2008
http://lhcb-doc.web.cern.ch/lhcb-doc/presentations/conferencetalks/2008.htm
http://lhcbdoc.web.cern.ch/lhcbdoc/presentations/conferencetalks/postscript/2008presentations/Schmidt%20pcdgs.pdf

[12]
S.O.Rice
Mathematical analysis of random noise
Bell System Technical Journal 24 (1945) 46–156

[13]
W.Riegler
http://riegler.home.cern.ch/riegler/sensitivity.htm

[14]
G.Auriema
1st LHCb Collaboration Upgrade Workshop, 12 January 2007
http://indico.cern.ch/getFile.py/access?contribId=20&sessionId=13&resId=0&materialId=slides&confId=8351

[15]
G.Martellotti, R.Nobrega, E.Fufaro, G.Penso, D.Pinci
Study of the performance of the LHCb MWPC with cosmic rays
CERN-LHCb-2008-057

[16]
R.Nobrega
Threshold Scan Analysis; Tool and Results (15/06/2009 Electronic logbook, record 534)
http://indico.cern.ch/getFile.py/access?contribId=15&sessionId=0&resId=2&materialId=slides&confId=48958

[17]
Bochin, B; Guets, S; Lazarev, V A; Saguidova, N; Spiridenkov, E M; Vorobev, A; Vorobyov, A
Beam tests of WPC-7 prototype of wire pad chambers for the LHCb muon system
LHCb-2000-102.

[18]
Anelli, M; Ciambrone, P; Felici, G; Forti, C; Lanfranchi, G; Rosellini, R; Santoni, M; Saputi, A; Sarti, A; Sciascia, B
Test of a MWPC for the LHCb Muon System at the Gamma Irradiation Facility at CERN
CERN-LHCb-2005-003

[19]
W.Riegler
CARIOCA Review Final
http://lhcb-muon.web.cern.ch/lhcb-muon/electronics/electronics.htm

[20]
Kashchuk, A ; Levitskaya, O ; Mair, K ; Nobrega, R ; Schmidt , B ; Shatalov, P ; Schneider, T
Pre-installation tests of the inner-most MWPCs for the LHCb Muon system
CERN-LHCb-INT-2009-010

[21]
R.Santacesaria, et al.
http://indico.cern.ch/getFile.py/access?contribId=0&resId=1&materialId=slides&confId=58893

[22]
A.Kashchuk
MWPC conditioning technique
http://kashchuk.web.cern.ch/kashchuk/LHCb/note2005-096muon.pdf
http://indico.cern.ch/getFile.py/access?contribId=0&resId=1&materialId=slides&confId=26114

[23]
J.-S. Graulich, H.-J. Hilke, A. Kachtchouk, K. Mair, B. Schmidt, T. Schneider
Conditioning of MWPCs for the LHCb Muon System
2005 IEEE Nuclear Science Symposium and Medical Imaging Conference
San Juan, Puerto Rico; October 23-29, 2005
http://lhcb-doc.web.cern.ch/lhcb-doc/presentations/conferencetalks/2005.htm

[24]
I.Smirnov
Modeling of ionization produced by fast charged particles in gases
Nuclear Instruments and Methods in Physics Research A 554 (2005) 474–493

[25]
J.A.Hornbeck,
Phys.Rev. 84(1951), 615-620

[26]
W.Bonivento, G.Manca
Measurement of the logical pad cluster size of the installed muon chambers with the 2008 cosmic runs
CERN-LHCb-2009-031
http://cdsweb.cern.ch/record/1163365/files/LHCb-2009-031.pdf

Appendix

Table A1.

Measurements presented in ref.[16] are wrong, because systematically do not correspond to correct ENC derivatives, see e/pF (last column):
45e/pF for CARIOCA positive
42e/pF for CARIOCA negative
Such ENC cannot be used for threshold setting.

MWPC type	*Cdet (pF)*	*ENC (fC)*	*dENC/dC (e/pF)*
M2R1_DCRO	120	1,2	38,50
M2R1W	70	0,8	27,61
M2R2_SCRO	100	1	36,83
M2R2W	80	0,9	29,63
M2R3_SCRO	106	1,1	31,20
M2R4W	165	1,5	36,80
M3R1_DCRO	130	1,2	36,98
M3R1W	80	0,9	21,03
M3R2_SCRO	110	1,1	36,89
M3R2W	90	1	27,72
M3R3_SCRO	114	1,1	31,75
M3R4W	185	1,6	36,20
M4R1_SCRO	72	0,8	29,44
M4R2_SCRO	139	1,3	39,53
M4R3P	139	1,3	39,53
M4R4W	205	1,7	36,63
M5R1_SCRO	75	0,8	31,60
M5R2_SCRO	139	1,3	40,88
M5R3_SCRO	145	1,3	40,91
M5R4W	225	1,9	36,99

The reason of 'reduced *ENC*' and derivative *dENC/dC* can be explained by increased slope in vicinity of zero-threshold, as shown in Fig.A1. This phenomenon was discussed in ref.[3], as an evidence of a partial positive feedback in some channels of the system.

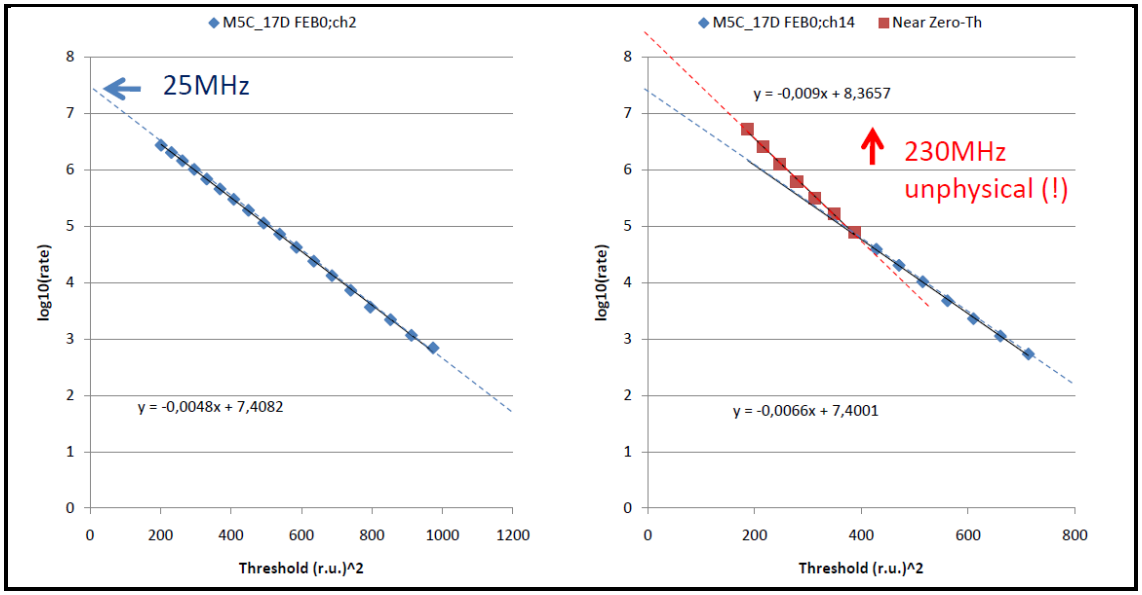

Fig.A1. Correct (left) and increased slope in vicinity of zero-threshold (right).

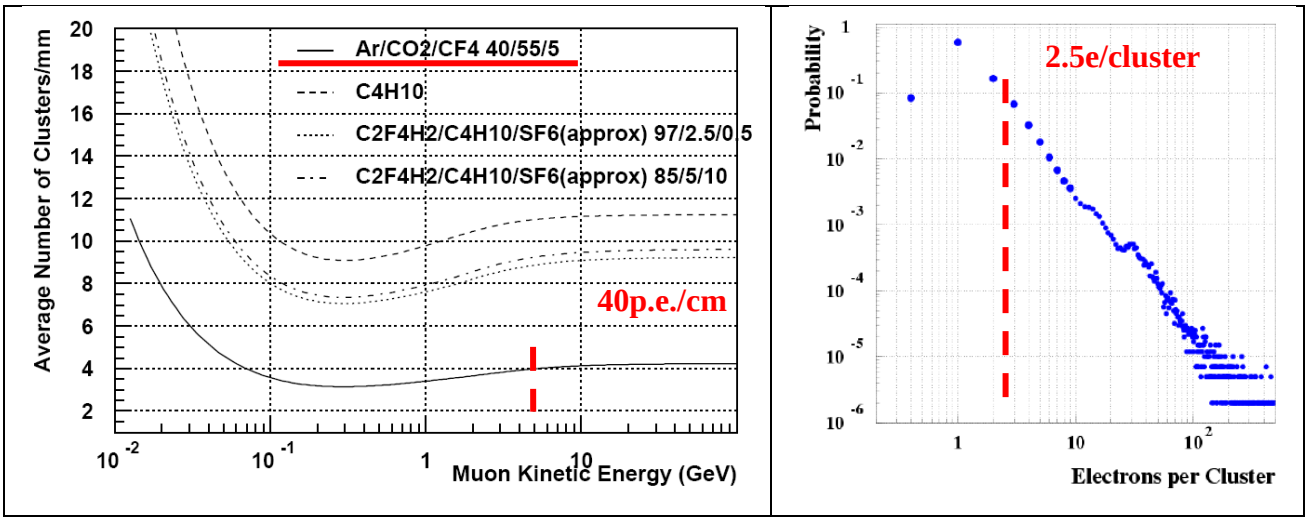

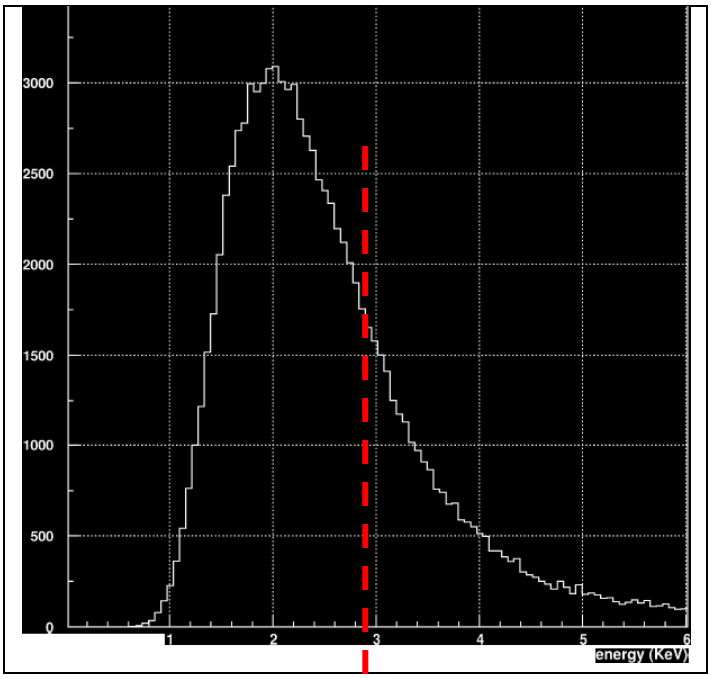

Fig.A2. Primary (top left), total (top right) ionization and distribution (bottom) of the created electrons with 97.3e in average and 66.7e the most probable obtained per 1cm by HEED [24] for the LHCb muon MWPC filled with gas mixture Ar(40%)/CO2(55%)/CF4(5%).
The vertical lines indicate our case.

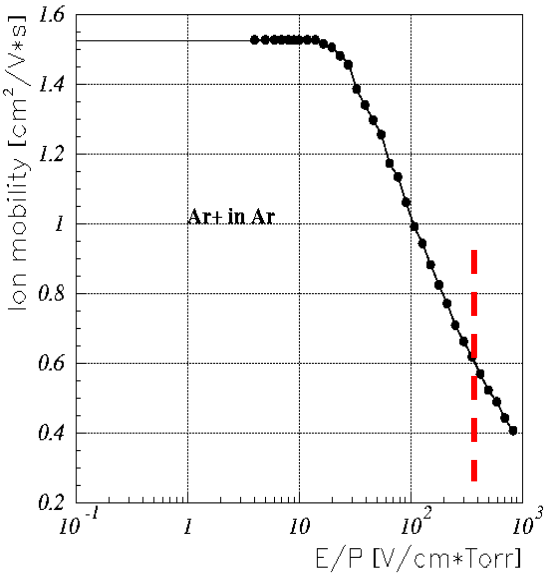

Fig.A3. Fraction of charge collected at T_p is defined by ion mobility $\mu(E)$ according to ref. [25] and equal to ~*10%* for LHCb muon MWPC, see *Eq.(A1)* for equivalent radius of cathode *b* and radius of anode wire *a*. The vertical line indicates our case.

Gas gain calculations in section 1.6 and Table 2 were made using *Eq.(A1)*:

$$G = \frac{1}{\delta} \cdot \frac{Th(e)}{Th(p.e.)}$$

$$\delta = \frac{\int_0^{T_P} i(t)dt}{\int_0^{T_c} i(t)dt} = \frac{\int_0^{T_P} \frac{dt}{t+t_0}}{\int_0^{T_c} \frac{dt}{t+t_0}} = \frac{\ln\left(\frac{T_p}{t_0}+1\right)}{\ln\left(\frac{T_c}{t_0}+1\right)} = \frac{\ln\left(\frac{T_P}{t_0}+1\right)}{2\ln\left(\frac{b}{a}\right)} \approx 10\%$$

$$t_0(E) = \frac{a}{2\mu \cdot E} \approx 3.5ns$$

$$T_c = t_0 \cdot \left(\frac{b}{a}\right)^2 - \textit{ion collection time} \qquad (A1)$$